

## INVESTIGATION OF TWO-PARAMETER APPROACH TO ASSESSMENT OF DEFECTS IN RESIDUAL STRESS FIELDS

Jack P Beswick<sup>1,2</sup>, Andrey P Jivkov<sup>1</sup>, Peter James<sup>2</sup>, Andrew H Sherry<sup>3</sup>

1. School of Mechanical Aerospace and Civil Engineering, University of Manchester
2. Amec Foster Wheeler (Clean Energy-Europe)
3. National Nuclear Laboratory

### ABSTRACT

Current structural integrity assessment procedures, R6 for example, provide advice on the inclusion of residual stresses and the effect of plasticity on such stresses via specific corrections to the fracture parameter,  $K_r$ . These approaches are conservative, as there are no established methods to accurately assess the interaction of residual stress and inelastic strains at a defect. Low-constraint geometries introduce substantial crack-tip plasticity, the effect of which on existing residual stresses needs to be understood better for reducing conservatism. The advice in R6 for less conservative assessment of low-constraint crack geometries is to use two-parameter approaches: defect assessments are carried out in the J-Q space, where J is the usual crack driving force and Q is used to quantify constraint.

This paper reports results from ongoing work investigating the applicability of two-parameter approaches to structural integrity assessments of low-constraint crack geometries in the presence of residual stresses. Specifically, numerical results showing the behaviour of SENB specimens are presented within the J-Q space. These are derived for different defect depths in various stress fields, including local residual stress, global equivalent plastic strains, and a combination of the two. A collation of previously published J-Q results, both numerical and experimental, are presented and compared to the relevant outcomes of the work. This work provides a basis for an experimental programme for determining fracture toughness loci in the two-parameter J-Q space. A brief description of this testing programme is also provided.

### INTRODUCTION

Each of the major forged components in nuclear reactor pressure vessels (RPVs) are joined together through a welding process. The process of welding introduces significant residual stresses within the structure, which are of major concern when assessing the integrity of the RPV. These residual stresses, those that are still present when the initial loading has been removed, are usually reduced through post weld heat treatment in the major RPV welds. In some transition welds, between the nozzles and primary pipework, however, this treatment is not possible so the residual stresses remain. These have significant effects on the effective cleavage fracture toughness of the materials within the structure (James et al. 2011). The cleavage fracture toughness of a material is its ability to resist fracture through transgranular cleavage, a brittle and catastrophic mode of failure, which makes it of significant interest throughout the life cycle of the RPV. The fracture toughness of RPV steels is not only affected by weld induced residual stresses, but damage induced through neutron irradiation, which leads to radiation hardening and embrittlement. Reduced temperatures, such as those experienced during plant shutdown, also increase the probability of cleavage fracture occurring (Margolin et al. 1999).

All of the above factors (residual stresses, radiation and temperature) have significant effects on the effective fracture toughness of a material because they alter the level of plasticity in the material. For entirely brittle, or linear-elastic materials (including ceramics and glass at room temperature), there are

validated fracture mechanics approaches used for defect assessment in structures, which are both relatively simple to carry out and fairly well validated through testing. This linear elastic fracture mechanics (LEFM) approach is also suitable for materials where the plastic zone around a crack is very small compared to the size of the uncracked ligament, known as small scale yielding (SSY) conditions. Where the effect of plasticity is not negligible more complex approaches such as elastic plastic fracture mechanics and local approaches to fracture are required to assess structural integrity.

The effects of both residual stress and plastic strain on cleavage fracture toughness are still not sufficiently well understood and their combined effects cannot be accurately characterised by a single parameter without undue conservatism. The current thinking is that a two-parameter approach including a parameter that quantifies a phenomenon known crack tip constraint may provide a more accurate and less conservative assessment; for example using J-Q two parameter fracture mechanics, where J is the usual crack driving force and Q quantifies constraint. In this framework an engineer can perform finite element analysis of the cracked geometry under a given loading condition, which may include a residual stress profile, to calculate J and Q. These calculations can then, it is proposed, be compared against a failure locus in the J-Q space to predict failure and assess the integrity of the structure around the defect.

One outstanding issue is to confirm that a unique material failure curve in the J-Q space exists for a specific RPV steel irrespective of the initial stress-strain conditions, geometry and loading. This requires that as many as possible failure points in the J-Q space are known and these are reached starting from different initial stress/plastic strain conditions. The underlying challenge is the limited knowledge of the effects of prior plasticity on cleavage fracture probability in general and of initial plastic deformations, when present, in particular. Progress towards developing new understanding of prior plasticity and residual stress on cleavage probability can be made by considering scenarios either with or without residual stress and or prior plasticity. This paper reports on the current progress of a research programme designed to investigate the existence of a unique material failure curve by undertaking a combination of numerical analysis and targeted experimental work with respect to the above scenarios.

## CRACK TIP CONSTRAINT

R6: the guideline for structural integrity assessments within nuclear power plants, describes constraint: “(A) material’s resistance to fracture is increased when specimens with shallow cracks, or specimens in tension, are tested. These conditions lead to lower hydrostatic stresses at the crack tip, referred to as lower constraint (R6 Panel, 2000).” It is apparent that this loss of constraint, which is affected by geometry and loading, as opposed to being a material property, has significant effects on the fracture resistance of certain components, especially where large-scale plasticity is observed. Due to this, two-parameter fracture toughness approaches have been developed, which quantify constraint for structural integrity approaches. O’Dowd and Shih (1991) suggested that the HRR (Hutchinson 1968) (Rice and Rosengren 1968) fields were insufficient to describe the stress field ahead of a crack tip where constraint is low. The Q parameter, as shown below, was postulated, which provides a comparison of the crack tip stresses parallel to the opening mode stress with those in a small scale yielding field, incorporating elastic-plastic effects (r is distance from the crack,  $\theta$  is the angle from the crack plane, and  $\sigma_0$  is a reference stress, usually taken as the yield stress of the material):

$$\sigma_{ij}(r\sigma_0/J, \theta) = \sigma_{ij}^{SSY}(r\sigma_0/J, \theta) + Q\sigma_0\delta_{ij} \quad [1]$$

This parameter is advocated in the R6 guidelines (R6 Panel, 2000) as valid for structural analysis of low constraint components. The calculation of Q is carried out through creating a boundary layer model loaded to a prescribed value of J or K. The boundary layer model simulates a semi-infinite crack in an infinite body, where theoretically there is no loss of constraint, and Q=0. This small scale yielding stress

field is then compared with the stress field at a normalised distance  $r\sigma_0/J=2$ , for the finite-geometry model under consideration. As the boundary layer model shows no loss of constraint, the current understanding is that almost all finite geometry specimens will lose constraint, and will have a negative Q (special cases exist however, including where bending occurs, where Q can increase slightly). Following the calculation of the Q value it is then possible to plot against the appropriate J value at which it is calculated. The purpose of this project is to populate such J-Q curves for both high and low constraint specimens. As explained previously this J-Q analysis will consider the effects of both residual stress and inelastic pre-straining on the J-Q curves.

## CURRENT J-Q FAILURE DATA

Prior to the commencement of experimental programme, it was decided to try and expand the current J-Q failure dataset based on fracture toughness failure data available for A533B steel. The work in this research programme is predominately associated with SENB specimens, which can show both high and low levels of constraint, depending on the crack depth to width ratio ( $a/w$ ). A fracture toughness testing programme of A533B was carried out in the 1990s, to investigate and validate SINTAP constraint procedures (Hadley and Karger, 1999). These included wide plate SENB tests (width=50mm), with varying crack depths, at  $-100^\circ\text{C}$ . The results were obtained from specimen tests that demonstrated no ductile tearing of greater than 0.2mm ahead of the crack prior to unstable fracture, which lends to the assumption they failed through cleavage. The failure data was presented in terms of the J-Integral as calculated based on the BS7910 procedure: a function of load on the specimen and crack-mouth opening displacement.

The results were interpreted into J-Q failure data using equation [1]. To achieve this 2D SENB specimen meshes were created in the commercial finite element software package ‘Abaqus’ (Dassault Systemes, 2013), with plane strain elements of unit thickness (CPEQR), with collapsible (single side, midside node position 0.25) elements at the crack tip, where the mesh was focussed to a minimum element size of  $5\mu\text{m}$ . The crack tip mesh is shown in Figure 1. The SENB loading was carried out through a 15mm radius loading pin displaced vertically into the specimens 2mm, with the only boundary conditions being symmetry ahead of the crack tip and fixing of the roller on which the specimen would rest (see Figure 4 for similar assembly schematic of 3D simulation). There was frictionless contact assigned to each of the appropriate surfaces. The material properties were taken directly from tensile test data of A533b steel at  $-90^\circ\text{C}$ , as data was not available at  $-100^\circ\text{C}$ . The software was programmed to calculate the J Integral at 100 increments in a single load step, such that a complete simulation of the fracture toughness test could be carried out. Due to the large number of specimens at varying levels of crack depths a python script was written to automatically construct the simulations. This code allowed each of the meshes to be created, and the input file for the jobs to be written automatically. It is planned that as the research in this programme progresses python scripts such as this will be written to create large numbers of Abaqus simulations to investigate J-Q the behaviour for different fracture toughness specimens based on available historical failure data, for both A533B and potentially other materials.

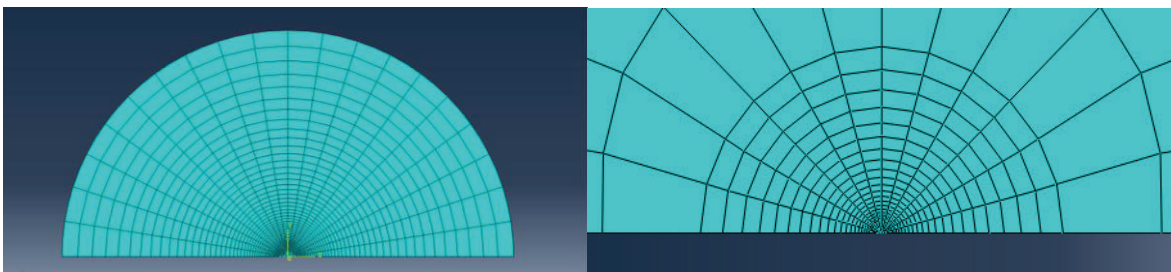


Figure 1: Boundary Layer Model and SENB Crack Tip Meshes

A second python script, here referred to as the JAQ code, was written to extract the J-Q results from the completed simulations. As the Q parameter was extracted at a normalised distance of  $r\sigma_0/J=2$ , it was first necessary to find the value of normalised stress at this distance from the small-scale-yielding field. This was achieved through the creation of a boundary layer model, to simulate a semi-infinite crack in an infinite body. The boundary layer model was created using the same elements and material properties as the SENB models, and was simply a semi-circle with a radius of 1m, whose mesh was again focussed at the crack tip as per the SENB model, to a minimum element size of  $5\mu\text{m}$  (see Figure 1). This model was subjected to displacement boundary conditions to a specified level of J around the outer circumference, and the normalised stress value was extracted at  $r\sigma_0/J=2$ . As the boundary layer model shows no loss of constraint, this value was taken as a constant through all increments of loading. This value was then subtracted from the normalised stress from the finite geometry simulations and J-Q results were extracted using the JAQ code, for each loading increment. From these results it was possible to extract the J-Q failure points for each of these simulations, based on the failure data in the literature (Hadley and Karger, 1999). Presented in Figure 2 are the results from the python scripting exercise. As can be seen it was possible to extract a large amount of data from the simulations that could then be used to populate a constraint based failure diagram with the results from the literature (Hadley and Karger, 1999).

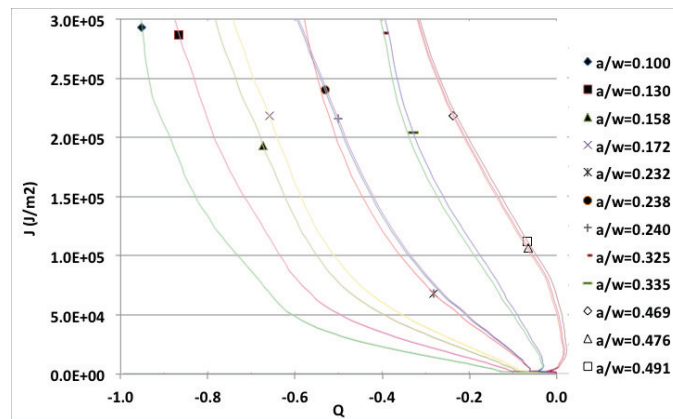


Figure 2: J-Q Failure Plot for Wide-Plate SENB Tests

The results here demonstrate some correlation between a reduction in Q and an increase in fracture toughness, although there is some experimental scatter visible. Although inconclusive as a failure curve with regards to any load history they lend weight to the existence of a failure curve in the J-Q space for this specific material in its virgin condition, at a single temperature. The results also demonstrate the significance of the JAQ code in that the data could be extracted automatically and easily from various simulations. The original report from which these data were extracted (Hadley and Karger, 1999) also presented the failure data in terms of J and Q, but comparison has been omitted with these results due to a lack of the material properties used in the original calculations, the actual tests were carried out at  $-100^{\circ}\text{C}$  and no tensile data at this temperature was available.

Hurlston (2011) has previously explored the effects of residual stress on the J-Q behaviour of A533B steel, and developed a fracture toughness curve, which is displayed in Figure 3. Hurlston's work focused on inducing residual stresses without inducing crack tip plasticity; achieved by local out of plane compression, through side punching an SENB specimen ahead of the crack. There follows details as to how the current work has expanded on these results through the incorporation of plastic strains into similar numerical simulations as those carried out by Hurlston, so as to expand the failure curve results following the experimental programme.

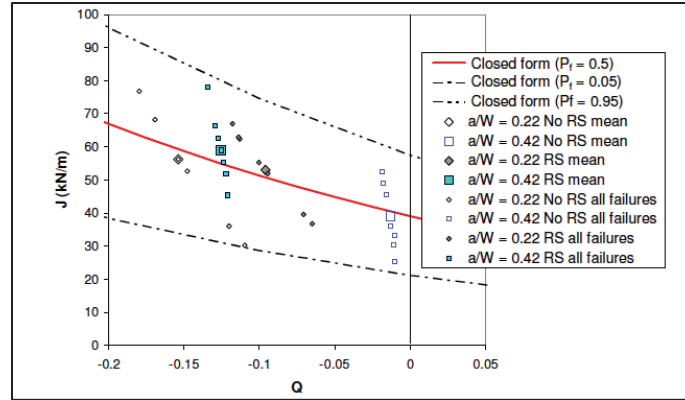


Figure 3: Fracture Toughness Curve in the J-Q Space for Two Cracks Depths ( $a/w=0.22, 0.42$ ) with and without Residual Stresses (RS).  $P_f$  denotes percentile of experimentally tested failures (Hurlston, 2011)

As can be seen the failure loads for these experiments were in general much lower than the results presented in Figure 2. These experiments took place at lower temperatures ( $-140^{\circ}\text{C}$ ) and therefore the material was closer to the lower shelf of the fracture toughness curve. Because of this it is difficult to compare the two sets of results, although these results are likely to prove more significant to the overall body of this work, as at these low temperatures cleavage fracture is most likely, so the planned experiments will be conducted at the same temperatures. What follows is details of the numerical investigation as to how Hurlston’s results have been built on to include global equivalent plastic strains within the increasing body of J-Q failure data this paper has collated.

### NUMERICAL SIMULATION OF SENB FRACTURE TOUGHNESS TESTS WITH RESIDUAL STRESS AND PLASTICITY

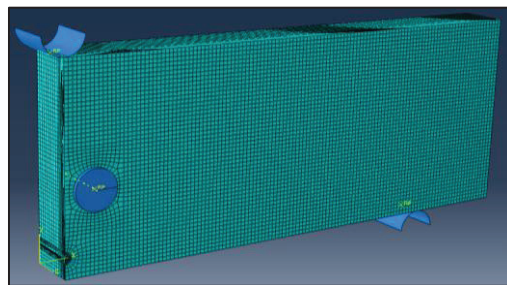


Figure 4: 3D Finite Element Assembly

Three-dimensional simulations were carried out to reproduce Hurlston’s work such that the interaction of plasticity with the residual stress field could be investigated in terms of J-Q behaviour. As per the 2D SENB finite element simulations described earlier in this work, 3D meshes were created and loaded similarly, with crack depths of  $a/w=0.1$  and  $0.5$ . It was decided to use different crack depths from the previous work to (a) introduce a broader scope to the J-Q failure curve and (b) introduce more extreme levels of high and low constraint. The simulations involved indenting a circular punch to the front of the specimens such that residual stress could be introduced ahead of the crack tip. This method was proven in Hurlston’s work to introduce significant tensile residual stresses that would appropriately simulate those experienced by defects close to a weld. The opening mode residual stress (S11) profiles are shown in Figure 5, where “Constrained” refers to the fact they are taken prior to any crack insertion (symmetry boundary conditions were applied behind the crack tip), and the neutron diffraction results refer to those stress measurements taken through neutron diffraction from the side-punched specimens, such that the

stress profiles could be compared ( $r$  refers to distance ahead of the crack). As can be seen there is relatively good agreement close to the crack tip between the two crack depths and the previous experimental data.

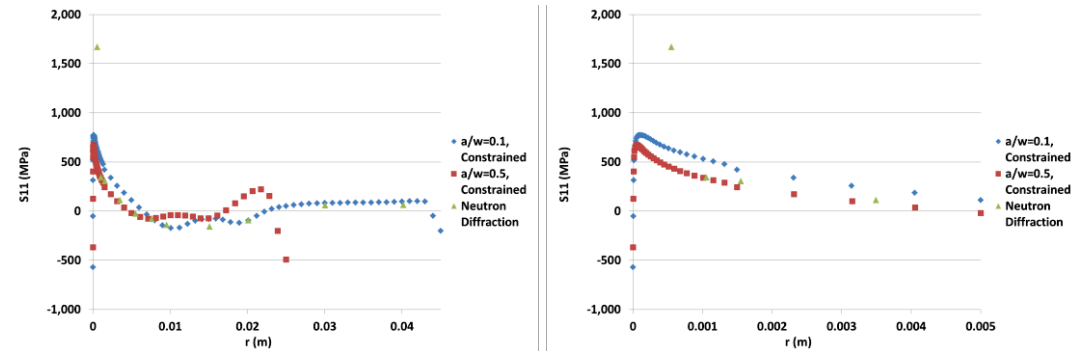


Figure 5: Opening Mode Residual Stress Profiles prior to Crack Insertion

The simulations involved, following residual stress induction, the insertion of a crack by removing the symmetry boundary conditions behind the crack, and then a subsequent cooling from the ambient temperature (material properties taken from tensile tests at 20°C), to the cryogenic temperatures at which the experiments will be carried out (material properties taken from tensile test data at -140°C). The specimen was loaded through pin displacement as with the 2D simulations. To simulate plasticity effects an equivalent plastic strain field was applied to the whole specimen, at the start of the simulation, at levels of 2, 5 and 10%, which were chosen to simulate strain levels that could be experienced in the heat affected zone of a weld, based on data in the literature (Smith, 2006). This led to 16 scenarios: 2 crack depths, with and without residual stress, at four levels of equivalent plastic strain (including 0%). The results were then processed using the JAQ code to provide the plot shown in Figure 6, where (R/NR denote residual stress/ no residual stress, 01 or 05 denotes crack depth, and H denotes level of equivalent plastic strain, or hardening so NR01H2 is no residual stress,  $a/w=0.1$ , with 2% equivalent plastic strain). Note the vertical axis begins at 10kJ/m<sup>2</sup>. This is because the JAQ code was programmed to start its calculations from the second contour, as the Abaqus user's manual (Dassault Systemes, 2013) concedes the  $J$  calculations at the first contour (or  $r=0$ ), are erroneous. This leads to a first reading of  $r\sigma_0/J=2$  at low loads, so it is impossible to calculate a  $Q$  value.

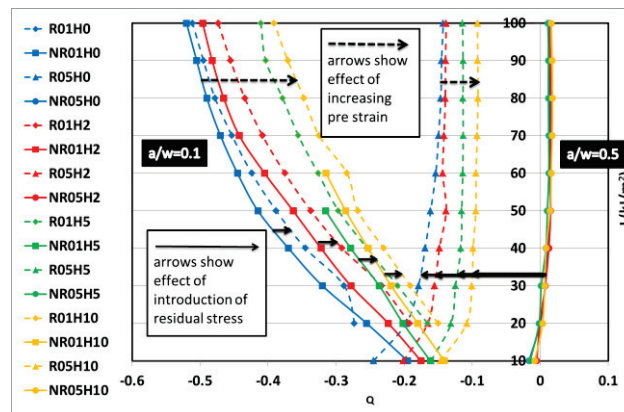


Figure 6: J-Q Plot for SENB Simulations with Residual Stress and Equivalent Plastic Strain

The plot raises several points for consideration. As can be seen to the right of the plot, which is a deep crack there is no significant change in the  $J$ - $Q$  behaviour through increase of pre-straining. At very high

constraint the global plasticity plays no real part in the Q results and this is to be expected: it can be said that near SSY yielding conditions prevail. However for the same very deep cracks where residual stress is involved it can be seen that initial plastic strains have an effect: if residual stresses are present Q increases with the hardness of the material.

At low constraint it can be seen that this effect is continued, there is a distinct increase in Q as the equivalent plastic pre-straining increases. Residual stress at these lower constraint conditions however serves to increase as opposed to decrease Q. Through observation of the results it appears possible that there are some geometrical (or loading) conditions where a switch occurs, such that above a specific load and/or crack depth the value of Q is reduced through the induction of residual stress. Then at lower values of a/w the residual stress serves to increase Q, meaning that residual stress is more of a concern for lower constraint cracks. This could be explained through the nature of stresses at the crack tip, with lower constraint specimens there are significantly lower opening mode crack tip stresses when compared to the small-scale yielding field. Therefore the opening mode tensile residual stress contribution is additive so increases the value of Q. At very high levels of constraint, where opening mode stresses are higher regardless of the relatively low opening mode residual stress, compressive interactions from the residual stress field appear to play a more significant role and may actually reduce the value of Q.

The Q values involving equivalent plastic pre-strain were calculated through comparison of a boundary layer model using the same level of pre-strain. This is an area of some debate as essentially these calculations become for a different material, the hardening field changes the material properties to further along the stress strain curve. The reference stress was also altered for the Q normalisations, to the yield stress at the new level of hardening. Initially the calculations were carried out with the SSY field with virgin material properties, although this led to positive Q values that contradict current theory. Furthermore the similarity of the high-constraint curves without residual stress validates these methods: one would expect very high constraint specimens to display this type of curve, in that there is little difference from the SSY field. This calculation method explains the increase in Q that is displayed in both the high and low constraint specimens, as the level of pre-strain increases, the material essentially becomes harder and more brittle, so Q increases. That said, this, alongside the method of calculating J, are areas of on going investigation throughout this work, and it is predicted that with experimental data more detailed physical explanations of the numerical results and validation of the calculations will be possible.

## **J IN THE PRESENCE OF RESIDUAL STRESSES**

Certain issues exist with the calculation of J in the conventional way as discovered by Rice (1968), using the finite element method, where initial inelastic or thermal strains are in the crack vicinity prior to loading or crack extension. One aspect of these inaccuracies is the difficulty involved in defining the stress, strain and strain energy density fields accurately close to the crack tip, necessary for the J calculation (Beardsmore, 2008). Another aspect of the problem with prior inelastic strains being incorporated into the model is that the path independence of the J integral relies on the stresses at the crack increasing in proportion with the loading, where “the different components of the stress tensor vary in constant proportion to one another and change monotonically with increase of the external load” (Lei, 2005). This is not necessarily true where initial strains are present, and render the accuracy of the J integral questionable. Works by Lei et al. (2000), Lei (2005), and Beardsmore (2008) offer modifications of Rice’s equation to enable the computation of the J Integral where the crack tip loading is non proportional and where inelastic strains are present before cracking.

The earlier work by Lei et al. (2000) offers modifications to the J calculation, which is incorporated into recent versions of Abaqus (Dassault Systemes, 2013), allowing users to compensate for residual stresses (strains). This adjustment splits the strain tensor  $\epsilon_{ij}$  into an initial (residual) strain  $\epsilon_{ij0}$  and an applied (mechanical) strain  $\epsilon_{ijm}$ .  $\epsilon_{ij0}$  remains as a constant through subsequent deformation and  $\epsilon_{ijm}$  increases with

stress as defined by the material's constitutive law. This allows the modification of the J integral to be defined to include initial strain, and remain path independent, where  $w$  is the mechanical strain energy density (see below), and  $A$  is the area surrounded by the contour  $\Gamma$  (Lei et al. 2000):

$$w = \int_0^{\varepsilon_{ij}^m} \sigma_{ij} d\varepsilon_{ij}^m \quad [2]$$

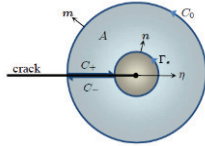
$$J = \int_{\Gamma} \left( w dy - \sigma_i \frac{\partial u_i}{\partial x} \right) n_i ds + \int_A \left( \sigma_{ij} \frac{\partial \varepsilon_{ij}}{\partial x} \right) dA$$

Equation [2] does not however, account for the non-proportional effects as described earlier. The non-proportional loading may lead to path dependence using these calculations rendering them inaccurate for calculations of J in the presence with initial strains. The later works by Beardsmore (2008) and Lei, J (2005) offer similar solutions for this issue. Their modifications remove the proportional assumptions through separation of the strain energy density ( $W$ ) term into the initial plastic strain energy density ( $W_{p0}$ ) and the mechanical ( $W_m$ ). Further separation of the strain into its constituent parts is also considered so the strains are separated into  $\varepsilon_{ij}^e$  (applied elastic),  $\varepsilon_{ij}^p$  (applied plastic),  $\varepsilon_{ij}^{p0}$  (initial plastic); and  $\varepsilon_{ij}^I$  (initial thermal, where applicable). This leads to:

$$\varepsilon_{ij}^* = \varepsilon_{ij}^{p0} + \varepsilon_{ij}^I \quad [3]$$

$$\varepsilon_{ij}^m = \varepsilon_{ij}^p + \varepsilon_{ij}^e - \varepsilon_{ij}^{p0}$$

Furthermore the contour region is again expanded over a longer path ( $C=\Gamma+C++C+C_0$ ) to allow for integration over an area as can be seen below, where  $q$  is a vector field= $\eta$  (a unit vector parallel with the crack tip) on  $\Gamma$  and  $0$  on  $C$ ,  $m_i$  is a unit vector parallel to  $C_0$ .



$$J = \oint_C W^m \delta_{ik} - \sigma_{ij} \left( \frac{\partial u_j}{\partial x_k} \right) m_i q_k ds \quad [4]$$

This equation was further expanded by Beardsmore (2008), using Green's theorem, for use in an Abaqus post-processing code know as JEDI (J-Equivalent Domain Integral):

$$J = \int_A \left\{ \left( \sigma_{ij} \left( \frac{\partial u_j}{\partial x_k} \right) - W^m \delta_{ik} \right) \frac{\partial q_k}{\partial x_i} - (M_k - E_k) q_k \right\} dA \quad [5]$$

$$M_k = \frac{\partial W^m}{\partial x_k} - \sigma_{ij} \frac{\partial \varepsilon_{ij}^m}{\partial x_k}$$

$$E_k = \sigma_{ij} \frac{\partial \varepsilon_{ij}^*}{\partial x_k}$$

Both Beardsmore, (2008) and Lei, (2005) proved that the above equations are suitable to be used to predict J for non-proportional loading under residual stress, in that the domain integrals remain path independent under these load history conditions. The JAQ code was modified such that the J integral as calculated by the JEDI software could be compared with those from Abaqus, to assess the effects of the non-proportional loading on J-Q behaviour. One scenario is in Figure 7 ( $a/w=0.5$ , with residual stress, equivalent plastic strain 10%). As can be seen there is very little alteration in the J-Q behaviour of the specimen over the loading span with which this research is concerned. This was observed over all numerically tested scenarios. That said it is still necessary to consider the non-proportional calculations

within this research, as although the J-Q curves adopt a similar shape (Figure 7, Left), the actual values of J corresponding to a specific value of Q, appear in a different position along the curve, which would alter the shape of the failure curve, as can be seen through the difference in J at the same load increment shown in Figure 7 (Right). Also, there is significant path dependence shown in the Abaqus results, which is removed through the JEDI method of calculating J with non-proportional loading. These discrepancies again demonstrate the importance of the JAQ software and its ability to alter different variables, enabling a thorough exploration and sensitivity analysis of the J-Q behaviour of the numerical simulations.

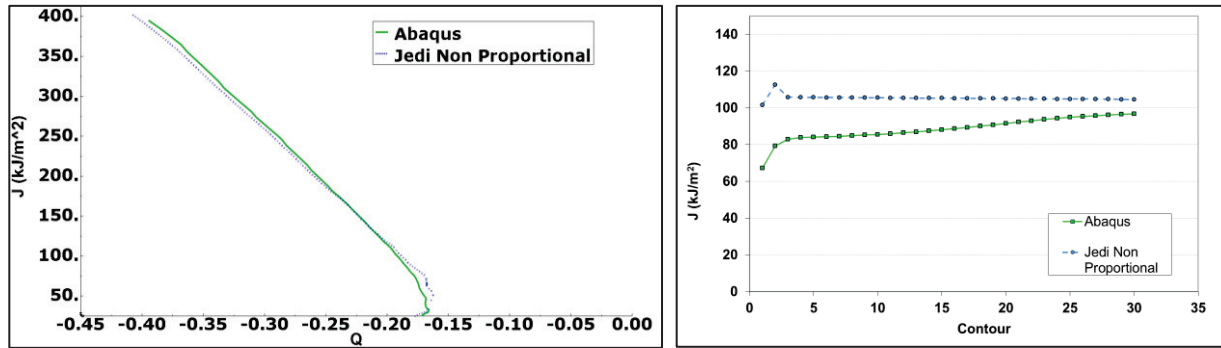


Figure 7: (Left) J-Q Calculations from Abaqus and JEDI Software, (Right) J Calculations across contour integral region at same increment of loading

## EXPERIMENTAL PLAN

The current plan is that full size SENB specimens (250 x 50 x 25mm) will be used for standard fracture toughness testing to be carried out at Amec Foster Wheeler in Risley, Warrington. The SENBs will have cracks fatigued in through vibrafre to levels of  $a/w=0.1$  and  $0.5$ . The residual stress will be induced, as per Hurlston's work through out of plane compression via double side punching, which has been proven and for which tooling is already prepared. The main outstanding issue to resolve is the induction of uniform equivalent plastic strain within the specimen. Parametric studies have been carried out using finite element simulations of a four-point-bend set up with the tooling and A533b plate dimensions available. It was found that although the plastic strains would not be uniform throughout the specimen, a level of equivalent plastic strain up to around 2% could be achievable through this method at the dimensions required. Although the repeated strain would not be uniform through the specimen, it is calculated that there would be large enough scale plasticity around the crack tip to enable experiments that would populate a failure curve, as this research programme requires. Furthermore the induction of tensile and compressive plastic strains into the material as would happen with four point bending, would enable a detailed evaluation of the microscopic effects on cleavage fracture, alongside the continuum effects observed in the J-Q behaviour.

## CONCLUSIONS

This paper has detailed the importance of better understanding the effects of the interaction of residual stress and global plasticity on crack tip constraint, and how their effects on cleavage fracture could reduce conservatism in structural integrity assessments of nuclear plant. A discussion of how constraint has been shown experimentally to affect fracture toughness in virgin materials and under the influence of residual stress has been presented. Several hypotheses, such as the effects of pre-straining on Q calculations, the physical effects of residual stress on constrain, and the non-proportional effects on the calculation of the J-Integral, have been presented, alongside an experimental plan into how to test the effects of the numerous variables considered, and how ultimately the results will be used to decide whether, when and how a material-specific failure curve could be used in structural integrity assessments. Most of the results

discussed in this work have been obtained using the JAQ code, a tool which has enabled quick and computationally cheap extraction of J-Q curves from both 2D and 3D simulations. The versatility of this code has been demonstrated through its integration with the JEDI software and it is likely that this code will be used throughout the remaining research programme to determine the most effective way of calculating the Q parameter, which has been shown to be open to some interpretation.

## ACKNOWLEDGEMENTS

The authors wish to acknowledge support (including a Nuclear EngD studentship) from the Engineering and Physical Sciences Research Council and Amec Foster Wheeler. They would also like to thank TWI, The University of Manchester, Dalton Nuclear Institute and EDF Energy for their continuing support with this project.

## REFERENCES

- Beardsmore, D. (2008) "JEDI: A Code for the Calculation of J for Cracks Inserted in Initial Strain Fields and the Role of J and Q in the Prediction of Crack Extension and Fracture." *ASME Pressure Vessels and Piping Division Conference*.
- Dassault Systemes. (2013) "Abaqus Analysis 6.13 User Guide."
- . "Abaqus Standard 6.13." (2013)
- . "Modeling Fracture and Failure with Abaqus." (2013)
- Hadley, I, and S Karger. (1999) "Effect of Crack Tip Constraint on Fracture Toughness of A533b Steel and Validation of the Sintap Constraint Procedure." *SINTAP/TWI/012*.
- Hurlston, R. (2011) "Development of Advanced Methods for Quantifying Fracture Toughness Properties in the Presence of Residual Stresses." EngD Thesis, University of Manchester.
- Hutchinson, J. W. (1968) "Singular behaviour at the end of a tensile crack in a hardening material" *Journal of the Mechanics and Physics of Solids* 16, 13–31.
- James, P., Hutchinson, P. and Madew, C. (2011) "Provisional Results for an Experimental Investigation into the Effect of Combined Primary and Secondary Stresses When Considering the Approaches of R6 and the recently Developed g() Factor." *ASME Conference on Pressure Vessels and Piping*.
- Lei, Y. (2005) "J Integral Evaluation for Cases Involving Non Proportional Stressing." *Engineering Fracture Mechanics* 72, no. 4: 577-596.
- Lei, Y, O'Dowd, N.P and Webster, G. A. (2000) "Fracture Mechanics Analysis of a Crack in a Residual Stress Field." *International Journal of Fracture*, no. 106: 195-216.
- Margolin, B Z, Shvetsova, V. A., and Gulenko, A. G. (1999) "Radiation embrittlement modelling for reactor pressure vessel steels: I. Brittle fracture toughness prediction." *International Journal of Pressure Vessels and Piping* 76: 715-729.
- O'Dowd, N P, and C F Shih. (1991) "Family of Crack-Tip Fields Characterized by a Triaxiality Parameter--I. Structure of Fields." *Journal of the Mechanics and Physics and Solids* 39, no. 8: 989-1015.
- R6 Panel (2000) "R6: Assessment of the Integrity of Structures Containing Defects" EDF Energy.
- Rice, J. R. and Rosengren, G. F. (1968) "Plane strain deformation near a crack tip in a power law hardening material" *Journal of the Mechanics and Physics of Solids* 16, 1–12.
- Rice, R (1968) "A Path Independent Integral and the Approximate Analysis of Strain Concentration and Cracks." *Journal of Applied Mechanics* 35: 379-386.
- Smith, M. (2006) "Hartlepool and Heysham 1 Power Stations: Development of mixed isotropic-kinematic material hardening models for finite element simulation of austenitic steel welds." *Engineering Division, British Energy*.